produces uniform Ohmic dissipation and uniform surface heat flux. The evidence is embodied in the excellent agreement between the measured temperature distributions along a vertically oriented, electrically heated foil and the analytical predictions for natural convection at a vertical plate with uniform surface heat flux.

This finding stands in contrast to ref. [1], where an intrinsically nonuniform heat flux was postulated to explain measured temperature distributions that were independent of the orientation of the heated foil, the mode of heat transfer, and various other factors. In further contrast, supplementary experiments performed here [3] indicated that the surface temperature distributions were highly sensitive to whether the foil was oriented vertically or horizontally. Furthermore, local voltage measurements did not reveal nonuniformities in the distribution of the electric current that appear to have existed in ref. [1].

REFERENCES

1. J. D. Tarasuk and G. S. P. Castle, Temperature distribution in an electrically heated wide metallic foil, *J. Heat Transfer* **105,** 210–212 (1983).
2. E. M. Sparrow and J. L. Gregg, Laminar free convection from a vertical plate with uniform surface heat flux, *Trans. Am. Soc. Mech. Engrs* **78,** 435–440 (1956).
3. C. K. Carlson, Natural convection from a uniformly heated horizontal surface shrouded above by a parallel, equi-dimension plate. Thesis, Department of Mechanical Engineering, University of Minnesota, Minneapolis, MN (1984).

Int. J. Heat Mass Transfer. Vol. 30, No. 3, pp. 604–607, 1987
Printed in Great Britain

0017-9310/87 $3.00+0.00
Pergamon Journals Ltd.

A heat balance integral method based on an enthalpy formulation

V. R. VOLLER

University of Minnesota, Mineral Resources Research Center, 56 East River Road, Minneapolis, MN 55455, U.S.A.

(*Received* 31 *October* 1985 *and in final form* 9 *April* 1986)

1. INTRODUCTION

THE HEAT balance integral (HBI) method developed by Goodman [1] is a useful engineering tool which can give a quick estimate of parameters associated with a diffusion-driven phase change. Many extensions and refinements to Goodman's method have been presented. Two important examples are: Hills [2], who developed the method for metallurgical applications; and Bell [3], who coupled finite-element concepts with the Goodman technique to develop a method which can give very high accuracy.

Goodman's HBI method is based on the Stefan formulation of a one-dimensional phase change. This involves satisfying a heat balance condition at an isothermal phase-change boundary. In some ways this represents a drawback in that many practical problems have the phase change taking place over a temperature range, e.g. the solidification of a binary alloy [4]. If this so-called 'mushy' region is significant then the Goodman HBI method may not be suitable. Recently Voller [4] has developed a heat balance integral method based on an enthalpy formulation for the analysis of a binary alloy. The aim of this paper is to generalise and investigate some aspects of this technique. In particular the performance of the enthalpy heat balance integral (EHBI) will be compared with previous HBI methods in the solution of: (i) a limiting case of a mushy region solidification; and (ii) a one-dimensional, isothermal one-phase Stefan problem.

2. BASIC PRINCIPLES—A MUSHY SOLUTION

The basic principles of the EHBI can be outlined on considering the following phase-change problem. Liquid initially at temperature $T = \varepsilon$ fills the positive half space $x > 0$, the liquid is such that it undergoes a liquid/solid phase change between temperatures $T = \varepsilon$ and $T = -\varepsilon$ with a loss of latent heat L. At time $t = 0$ the surface temperature at $x = 0$ is lowered to a temperature $T = T_0 < -\varepsilon$ in order that the phase change commences. The state of the system at time $t > 0$ is shown in Fig. 1. If the thermal properties are constant and heat conduction is taken as the only mechanism of heat transfer the following governing equations may be derived.

$$\frac{\partial}{\partial t}[T+H/C] = \kappa\frac{\partial^2 T}{\partial x^2} \tag{1}$$

the enthalpy formulation, where

$$H/C = \begin{cases} 0 & -\varepsilon > T \\ F(T)\alpha & -\varepsilon \leqslant T \leqslant \varepsilon \\ \alpha & T > \varepsilon \end{cases} \tag{2}$$

$\alpha = L/C$ and $F(T)$ is some function of temperature T which determines the nature of the phase change in the mushy region. Note that $F(\varepsilon) = 1$ and $F(-\varepsilon) = 0$.

The basic HBI approach is to approximate the temperature profile in the intervals $[0, X_0]$ and $[X_0, X_1]$ (see Fig. 1) by the quadratic profiles

$$\begin{aligned} U_0 &= T_0 - \frac{x}{X_0}(T_0+\varepsilon) + a_0 x\left[1-\frac{x}{X_0}\right] \\ U_1 &= -\varepsilon + 2\varepsilon\frac{(x-X_0)}{X_1-X_0} + a_1(x-X_0)\left[1-\frac{(x-X_0)}{(X_1-X_0)}\right]. \end{aligned} \tag{3}$$

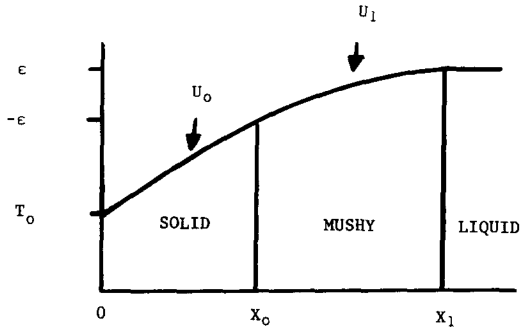

FIG. 1. State of freezing system at time t and showing approximating profiles.

NOMENCLATURE

C	specific heat
E	% relative error
$F(T)$	latent heat change with temperature
H	enthalpy
K	conductivity
k	partition ratio
L	latent heat
St	Stefan number, $-\alpha/T_0$
T_0	surface temperature
T_F	fusion temperature
T_L	liquidus temperature
U, U_0, U_1	temperature profiles
X, X_0, X_1	position of phase-change isotherms
Z_0, Z_1	non-dimensional space variables.

Greek symbols

α	ratio of L/C
ε	width of mushy zone
κ	diffusivity, $K/\rho C$
λ	parameters for isotherm movement
ρ	density.

Note that these profiles satisfy the temperature conditions at $x = 0$, X_0 and X_1. The values of a_0 and a_1 are found on setting

$$\frac{\mathrm{d}U_0}{\mathrm{d}x} = \frac{\mathrm{d}U_1}{\mathrm{d}x} \quad \text{at} \quad x = X_0$$

and

$$\frac{\mathrm{d}U_1}{\mathrm{d}x} = 0 \quad \text{at} \quad x = X_1$$

i.e. a continuity of flux condition. This gives

$$a_1 = \frac{2\varepsilon}{X_1 - X_0} \quad \text{and} \quad a_0 = -\frac{(T_0 - \varepsilon)}{X_0} - \frac{4\varepsilon}{X_1 - X_0}. \tag{4}$$

In a similar manner to Goodman, as implemented by Bell [3], equation (1) may be integrated over the two regions $[0, X_0]$ and $[X_0, X_1]$ to give, on substitution of the approximating polynomials

$$\frac{\mathrm{d}}{\mathrm{d}t}\left[X_0 \int_0^1 U_0\,\mathrm{d}Z_0 + \varepsilon X_0\right] = \kappa\left[\left(\frac{\partial U_0}{\partial x}\right)_{X_0} - \left(\frac{\partial U_0}{\partial x}\right)_0\right]$$

$$\frac{\mathrm{d}}{\mathrm{d}t}\left[(X_1 - X_0)\int_0^1 U_1\,\mathrm{d}Z_1 + \alpha(X_1 - X_0)\int_0^1 F(Z_1)\,\mathrm{d}Z_1\right.$$

$$\left. -(\alpha+\varepsilon)X_1 - \varepsilon X_0\right] = \kappa\left[\left(\frac{\partial U_1}{\partial x}\right)_{X_1} - \left(\frac{\partial U_1}{\partial x}\right)_{X_0}\right] \tag{5}$$

where

$$Z = \frac{x}{X_0} \quad \text{and} \quad Z_1 = \frac{x - X_0}{X_1 - X_0}.$$

On noting that U_1 is a function of Z_1 it follows that

$$A = \int_0^1 F(Z_1)\,\mathrm{d}Z_1$$

is constant with respect to time and equation (5) leads to

$$\frac{\mathrm{d}}{\mathrm{d}t}\left[\frac{X_0}{3}[T_0+\varepsilon] - \frac{2\varepsilon}{3}\frac{X_1^2}{(X_1 - X_0)}\right] = \kappa\left[\frac{2(T_0+\varepsilon)}{X_0} + \frac{8\varepsilon}{X_1 - X_0}\right]$$

$$\frac{\mathrm{d}}{\mathrm{d}t}\left[\frac{(X_1 - X_0)}{3}\varepsilon + \alpha(X_1 - X_0)A - (\alpha+\varepsilon)X_1 - \varepsilon X_0\right]$$

$$= \kappa\left[\frac{-4\varepsilon}{X_1 - X_0}\right] \tag{6}$$

two ODEs in $X_1(t)$ and $X_0(t)$. On letting

$$X_0 = \lambda_0\sqrt{\kappa t} \quad \text{and} \quad X_1 = \lambda_1\sqrt{\kappa t} \tag{7}$$

equation (6) gives a coupled non-linear system in parameters λ_1 and λ_0

$$\frac{\lambda_0}{6}[\mathrm{T}_0+\varepsilon] - \frac{\varepsilon\lambda_0^2}{3(\lambda_1 - \lambda_0)} = \frac{2(T_0+\varepsilon)}{\lambda_0} + \frac{8\varepsilon}{\lambda_1 - \lambda_0}$$

$$\frac{(\lambda_1 - \lambda_0)}{6}\varepsilon + \frac{\alpha(\lambda_1 - \lambda_0)}{2}A - \frac{(\alpha+\varepsilon)}{2}\lambda_1 - \frac{\varepsilon}{2}\lambda_0 = \frac{-4\varepsilon}{\lambda_1 - \lambda_0}. \tag{8}$$

When the nature of the phase change in the mushy region is such that the relationship $F(T)$, in equation (2), is known, equation (8) may be solved, for any given values of T_0 and ε, and explicit expressions for the isotherm movements and temperature obtained.

Analysis methods for mushy region phase change have been proposed previously. Tien and Geiger [5] employ an analytical solution in the solid phase and a HBI technique in the mushy phase. In the discussion of this paper Goodman [6] proposes a complete analytical solution for a mushy region phase change. Both these techniques are limited, however, in that the solid fraction temperature relationship is restricted to be of the form

$$F = (1 - Z_1) \tag{9}$$

where as in the proposed method, equation (8), the form of F is completely general. Nevertheless, the methods of Tien and Geiger [5] and Goodman [6] provide a means of investigating the applicability of equation (8). With the form of F given by equation (9), the value of A, in equation (8), becomes 1/2. Predictions using the EHBI are compared with predictions from the Tien and Geiger HBI (TGHBI) and the analytical solution (TRUE) for various values of Stefan number ($St = -\alpha/T_0$) and mushy half range ε in Table 1. From these results it may be observed that the proposed EHBI method performs well and produces results of a similar standard to those of the Tien and Geiger technique. As mentioned above, however, the proposed technique has a much greater flexibility in the choice for the form of $F(T)$. For example, Voller [4] has used the EHBI with success, to investigate the solidification behavior of a binary alloy where

Table 1. Comparison of methods and analytical solution

Values	Method	λ_0	λ_1
$\varepsilon = 0.1$ $St = 1.0$	EHBI	1.0278	1.5508
	TGHBI	1.0058	1.5364
	TRUE	1.0069	1.5310
$\varepsilon = 0.5$ $St = 1.0$	EHBI	0.4251	2.1644
	TGHBI	0.4226	2.1642
	TRUE	0.4297	2.1045
$\varepsilon = 0.25$ $St = 2.5$	EHBI	0.5400	1.2868
	TGHBI	0.5357	1.2851
	TRUE	0.5429	1.2470
$\varepsilon = 0.1$ $St = 5.0$	EHBI	0.5221	0.7622
	TGHBI	0.5188	0.7600
	TRUE	0.5209	0.7519
$\varepsilon = 0.5$ $St = 5.0$	EHBI	0.2387	1.2007
	TGHBI	0.2388	1.2007
	TRUE	0.2495	1.1144

Table 2. Comparison of cubic profile HBI methods

St	Analytical	Goodman	Cubic	Quad
1	1.24013	1.24706	1.23398	1.27299
5	0.612848	0.613098	0.612667	0.61744
10	0.440033	0.440082	0.439998	0.44177
20	0.313642	0.313651	0.313636	0.314278
50	0.199338	0.199339	0.199338	0.199503

the $F(T)$ relationship is given by the Scheil equation [7]

$$F(T) = \left[\frac{T_F - T}{T_F - T_L}\right]^{1/(1-k)}$$

where T_F is the fusion temperature of the pure material, T_L is the liquidus temperature of the binary alloy and k is the partition constant. When Tien and Geiger [8] use the Scheil equation their technique requires that F is approximated by a polynomial in Z_1 of order 10. This introduces considerable extra complications and computations into the analysis.

3. AN ISOTHERMAL, ONE-PHASE STEFAN PROBLEM

A further check on equation (8) can be achieved on taking the limit as $\varepsilon \to 0$, i.e. considering an isothermal temperature phase change. In the limit $\varepsilon \to 0$, $\varepsilon/(\lambda_1 - \lambda_0) \to \alpha\lambda/8$ and equation (8) reduces to the single quadratic

$$\lambda^4 + \lambda^2(24 + 4/St) - 48/St = 0 \qquad (10)$$

where $\lambda_1 = \lambda_0 = \lambda$. An alternative EHBI analysis using cubic temperature profiles in place of the quadratic profiles [see equation (3)] results in an almost identical equation, namely

$$\lambda^4 + \lambda^2(24 + 6/St) - 48/St. \qquad (11)$$

Equation (10) or (11) will predict the movement of the phase-change isotherm, X, for a one-phase Stefan problem from

$$X(t) = \lambda\sqrt{\kappa t}.$$

In this case there is also an analytical solution for λ obtained on solving

$$\sqrt{\pi}\lambda \exp(\lambda^2/4)\,\mathrm{erf}(\lambda/2) = 2/St. \qquad (12)$$

In addition Goodman [1] using a 'standard' HBI with a cubic profile derives the following cubic in λ^2

$$\lambda^6 + 36\lambda^4 + \lambda^2(288 + 24/St) - 576/St = 0. \qquad (13)$$

Comparison between the analytical solution, equation (12) and predictions of equations (10) [quad], (11) [cubic], and (13) [Goodman] is made in Table 2. These results indicate that

- the cubic EHBI gives more accurate results than the quadratic (note this does not mean to say that an increase in the order of the polynomial will always lead to improved accuracy);
- the accuracy of the cubic EHBI equation (11), is slightly better than that of the cubic Goodman HBI equation (13) note also that equation (11) (a quadratic) is easier to solve than equation (13) (a cubic);
- the cubic EHBI underpredicts whereas the cubic Goodman HBI overpredicts.

A possible reason for the difference between the Goodman HBI and the EHBI is in the boundary conditions used. In the Goodman HBI forcing the temperature profiles to satisfy the Stefan condition

$$\kappa \left.\frac{\partial T}{\partial x}\right|_X = \alpha \frac{\mathrm{d}X}{\mathrm{d}t} \qquad (14)$$

which expresses the heat balance at the phase-change isotherm, is a fundamental step. Whereas in the EHBI methods this condition is not explicitly involved. However an analysis of the EHBI shows that as $\varepsilon \to 0$ the Stefan condition *is satisfied* by the resulting profiles. For example, consider the EHBI quadratic profile, equation (3). In the limit $\varepsilon \to 0$ the solid profile becomes

$$U_0 = T_0 - \frac{x}{X}T_0 + a_0 x\left(1 - \frac{x}{X_0}\right)$$

where $a_0 = -T_0/X - \alpha\lambda/2\sqrt{\kappa t}$ which on substitution will satisfy the Stefan conditions, equation (14). Clearly more analysis is required to determine why the Goodman HBI and EHBI cubic methods differ.

4. CONCLUSIONS

HBI methods have proved to be a popular means of obtaining quick and accurate estimates of phase-change parameters. A practical drawback of such an approach is that only isothermal phase-change problems or problems with a restricted form of mushy region can be dealt with. In this paper an alternative HBI method was developed based on the enthalpy formulation of phase change. This method can deal with problems in which the phase change occurs over a temperature range, ε, the latent heat evolved expressed as a function of temperature $F(T)$. Furthermore:

- There is no restriction on the form of the $F(T)$ relationship.
- As far as isothermal phase changes are concerned (i.e. in the limit $\varepsilon \to 0$) predictions of the EHBI were in general more accurate than previous HBI techniques. In addition the form of the resulting equations were of a simpler form (i.e. quadratics as opposed to cubics).
- Analysis of the temperature profiles derived from the EHBI show that the profiles satisfy the Stefan heat balance of an isothermal phase change regardless of the fact that in the derivation of the profile *no* heat balance conditions were explicitly satisfied.

The EHBI approach outlined in this paper should prove useful in extending the range of problems to which HBI techniques can be applied. In fact, as previously mentioned, the technique has been successfully modified and applied to a problem of undirectional solidification of a binary alloy [4].

REFERENCES

1. T. R. Goodman, The heat balance integral and its application to problems involving a change of phase, *Trans. Am. Soc. mech. Engrs* **80**, 335–342 (1958).
2. A. W. D. Hills, A generalised integral profile method for the analysis of undirectional heat flow during solidification, *Trans. metall. Soc. A.I.M.E.* **245**, 1471–1479 (1969).
3. G. E. Bell, A refinement of the heat balance integral

method applied to a melting problem, *Int. J. Heat Mass Transfer* **21,** 1357–1362 (1978).
4. V. R. Voller, A heat balance integral method for estimating practical solidification parameters, *IMA J. appl. Math.* **35,** 223–232 (1986).
5. R. H. Tien and G. E. Geiger, A heat-transfer analysis of the solidification of a binary eutectic system, *J. Heat Transfer* **89,** 230–234 (1967).
6. T. R. Goodman, Discussion on a heat-transfer analysis of the solidification of a binary eutectic system, *J. Heat Transfer* **89,** 233–234 (1967).
7. M. C. Flemings, *Solidification Processing.* McGraw-Hill, New York (1974).
8. R. H. Tien and G. E. Geiger, A unidimensional solidification of a binary eutectic system with a time-dependent surface temperature, *J. Heat Transfer* **90,** 27–31 (1968).

Int. J. Heat Mass Transfer. Vol. 30, No. 3, pp. 607–610, 1987
Printed in Great Britain

0017-9310/87 $3.00+0.00
Pergamon Journals Ltd.

Mass transfer to an accelerating multidrop system

S. Ramachandran, C. Kleinstreuer† and E. R. Altwicker‡
Department of Mechanical and Aerospace Engineering, North Carolina State University, Raleigh, NC 27695-7910, U.S.A.

(*Received* 13 *February* 1986 *and in final form* 23 *July* 1986)

1. INTRODUCTION

A DETAILED analysis of the dynamics and transport mechanisms of interacting drops is important for the basic understanding of (dense) spray processes and for a variety of absorption, drying, cooling and combustion systems. In *dense* sprays, drops are so closely spaced that they interact with each other and thereby modify the local ambient conditions including drop dynamics, fluid properties and heat/mass transfer rates. Of particular interest here are the momentum and mass transfer with chemical reaction of accelerating and interacting drops on a one-dimensional trajectory at moderate to high Reynolds numbers, i.e. the range of $50 < Re < 400$. The lower limit allows the use of boundary-layer type postulates and the upper bound is given by the sphericity assumption of liquid drops.

Recent reviews of theoretical and experimental modeling results for predominantly combustion sprays have been contributed by Sirignano [1], Faeth [2], Law [3] and Bracco [4]. For example, Tal and Sirignano [5] and Tal *et al.* [6] discussed the fluid mechanics and heat transfer for sphere arrays using their cylindrical cell model which is an improvement over the classical spherical cell model due to Happel [7]. The drop spacing is given by the 'voidage' of the sphere assemblage where each sphere is in a fixed position surrounded by a rectangular cell. Since the voidage is directly related to the inter-drop distance, the lumped parameter effects of different geometric array parameters can be evaluated. However, the interaction dynamics of several individual drops and hence distributed parameter effects cannot be calculated. Bracco [4] reviewed mathematical models and supportive experimental data for engine sprays considering droplet break up, dense spray and dilute spray regions. Bracco and co-workers used the discrete droplet model (DDM) with appropriate probability density functions to study for dense sprays the effect of void fraction on interphase transport rates (which was found to be weak) and the effect of drop collisions on drop size increase (which was found to be significant). These modeling approaches result in average system parameters, i.e. no details of the velocity/pressure and concentration fields around or within individual, interacting drops can be extracted. On the other hand, statistical models are computationally very cost-effective in estimating integral properties of entire spray regions.

In this paper we concentrate on several spherical monodispersed drops which interact while falling through a polluted environment. The work is based on a series of previously published papers [8–10] which concentrated on absorption of a trace gas (e.g. sulfur dioxide) by gravity sprays.

2. MATHEMATICAL FORMULATION

A mathematical model is developed to simulate the mass transfer characteristics of a multidrop system, falling vertically on a one-dimensional trajectory. Based on a previous analysis [11], five drops are being considered to calculate the drop dynamics, followed by a three-drop analysis of mass transfer, i.e. trace gas absorption with liquid phase chemical reaction.

2.1. *Drop dynamics*

The following analysis is based on the assumptions that:

(a) monosized drops are released with the same initial velocity at a regular time interval, i.e. at constant frequency; possible drop coalescence is presently not considered;

(b) the acceleration/deceleration phase of the first three drops is of major interest;

(c) a drop inbetween neighboring drops will experience both a 'front sphere effect' and a 'back sphere effect' as has been experimentally observed [15, 16]; the average of these effects is experienced by the center drop;

(d) in focusing basically on the first three drops, the development of the air entrainment corridor [8] is not treated separately but included in a modified approach velocity and the wake velocity field for mass transfer.

The governing equation for the motion of the ith drop is Newton's second law which can be written as

$$\frac{\mathrm{d}v_i}{\mathrm{d}t} = g\left(1-\frac{\rho_a}{\rho_p}\right) - \frac{3}{8}\frac{C_{D,i}}{a}\frac{\rho_a}{\rho_p}v_i^2; \quad i = 1, \ldots, 5. \quad (1)$$

At any time, the dimensionless drop distance can be calculated from

$$d_{j,j+1} = (x_j - x_{j+1})/a; \quad j = 1, \ldots, 4 \quad (2)$$

where

$$\mathrm{d}x_i/\mathrm{d}t = v_i. \quad (3)$$

Based on the semi-empirical expressions given by Rowe and Henwood [12], the following equations are proposed for the

---

† To whom all correspondence should be addressed.

‡ Department of Chemical and Environmental Engineering, RPI, Troy, NY, U.S.A.